

Triarylboron-Based Fluorescent Organic Light-Emitting Diodes with External Quantum Efficiencies Exceeding 20 %

Katsuaki Suzuki, Shosei Kubo, Katsuyuki Shizu, Tatsuya Fukushima, Atsushi Wakamiya, Yasujiro Murata, Chihaya Adachi, and Hironori Kaji*

Abstract: Triarylboron compounds have attracted much attention, and found wide use as functional materials because of their electron-accepting properties arising from the vacant p orbitals on the boron atoms. In this study, we design and synthesize new donor–acceptor triarylboron emitters that show thermally activated delayed fluorescence. These emitters display sky-blue to green emission and high photoluminescence quantum yields of 87–100 % in host matrices. Organic light-emitting diodes using these emitting molecules as dopants exhibit high external quantum efficiencies of 14.0–22.8 %, which originate from efficient up-conversion from triplet to singlet states and subsequent efficient radiative decay from singlet to ground states.

Triarylboron (TAB) compounds have a vacant p-orbital on the central boron atom so they possess attractive electron-accepting properties. Donor-acceptor (D-A) systems with a TAB acceptor and amine-based donor groups have received considerable interest because of their strong intramolecular charge transfer (ICT) properties.^[1–5] The ICT character of TAB-based D-A compounds strongly influences their photo-physical and photochemical properties,^[1] and makes them useful for non-linear optics,^[2] anion sensing,^[3] hydrogen activation and storage,^[4] and optoelectronics.^[5]

However, a limited number of TAB D-A compounds have been used as emitters in organic light-emitting diodes (OLEDs) because the external quantum efficiency (η_{EQE}) of such devices has been relatively low.^[5a–f] One origin of the low η_{EQE} is spin statistics;^[6] conventional fluorescent materials can convert only 25 % of electrogenerated singlet excitons into light, and the remaining 75 % of generated triplet excitons are deactivated as heat. Considering that the light out-coupling efficiency of OLEDs is typically 20–30 %, ^[7] the theoretical

maximum η_{EQE} of OLEDs with conventional fluorescent emitters is limited to 5–7.5 %. Thus, efficient conversion of triplet excitons into light is needed to realize OLEDs with high η_{EQE} .

To extract light from triplet excitons, phosphorescent organometallic materials have been used as emitters in OLEDs.^[8] Phosphorescent organometallic emitters can theoretically convert 100 % of excitons to light because of strong spin–orbit coupling, so they have been frequently used in OLEDs.^[8c] Several TAB-based organometallic phosphorescent emitters have been reported.^[9]

Thermally activated delayed fluorescence (TADF) has recently been used as a different approach to acquire light from triplet excitons.^[10,11] TADF emitters, which often have D-A frameworks, can convert the lowest triplet excited state (T_1) to the lowest singlet excited state (S_1) through reverse intersystem crossing (RISC) by thermal activation.^[10,11] Although early TADF-based OLEDs showed relatively low η_{EQE} ,^[10] recent TADF emitters possess outstanding performance.^[11] The number of highly efficient TADF emitters is increasing rapidly at present, but is still small compared with the multitude of phosphorescence emitters. In particular, there are few reports of TAB-based TADF^[12] because it is still challenging to use versatile TAB-based D-A frameworks as TADF emitters, even though the strong π -electron accepting ability related to the p- π^* conjugation of TAB materials should be beneficial to realize TADF.

Herein, we report TAB-based TADF emitters **1–3** composed of an electron-accepting trimesitylboron analogue (Mes_3B) and three amine-based electron-donating units (Figure 1 a). OLEDs using **1–3** as emitting dopants exhibit high η_{EQE} of up to 22.8 %, far exceeding the theoretical limit for normal fluorescent emitters of 5–7.5 %. Specifically, the η_{EQE} of 21.6 % for a sky-blue OLED containing **2** is the highest value for a TADF-based blue OLED,^[13] while 22.8 % is the highest value for an OLED with a TAB emitter.

To realize efficient TADF emission, a very small energy gap between S_1 and T_1 (ΔE_{ST}) is required to promote RISC.^[11] ΔE_{ST} generally decreases when the exchange interaction between the highest occupied molecular orbital (HOMO) and lowest unoccupied molecular orbital (LUMO) of a molecule weakens.^[14] We selected the widely used Mes_3B unit as an electron-accepting segment,^[1–5] which has methyl groups at the *ortho* position of C–B bonds that protect the B atoms from oxygen and water. As the electron-donating unit, we used phenoxazine (PXZ), bis(diphenylamino)carbazole (2DAC), and diphenylaminocarbazole (DAC) units aiming to minimize ΔE_{ST} (Figure 1 a).

*] Dr. K. Suzuki, S. Kubo, Dr. K. Shizu, Dr. T. Fukushima, Prof. Dr. A. Wakamiya, Prof. Dr. Y. Murata, Prof. Dr. H. Kaji
 Institute for Chemical Research Kyoto University
 Uji, Kyoto 611-0011 (Japan)
 E-mail: kaji@scl.kyoto-u.ac.jp

Prof. Dr. C. Adachi
 Center for Organic Photonics and Electronics Research
 Kyushu University
 744 Motoooka, Nishi, Fukuoka 819-0395 (Japan)
 and
 Japan Science and Technology Agency (JST)
 Exploratory Research for Advanced Technology (ERATO)
 Adachi Molecular Exciton Engineering Project
 744 Motoooka, Nishi, Fukuoka 819-0395 (Japan)

Supporting information for this article is available on the WWW under <http://dx.doi.org/10.1002/anie.201508270>.

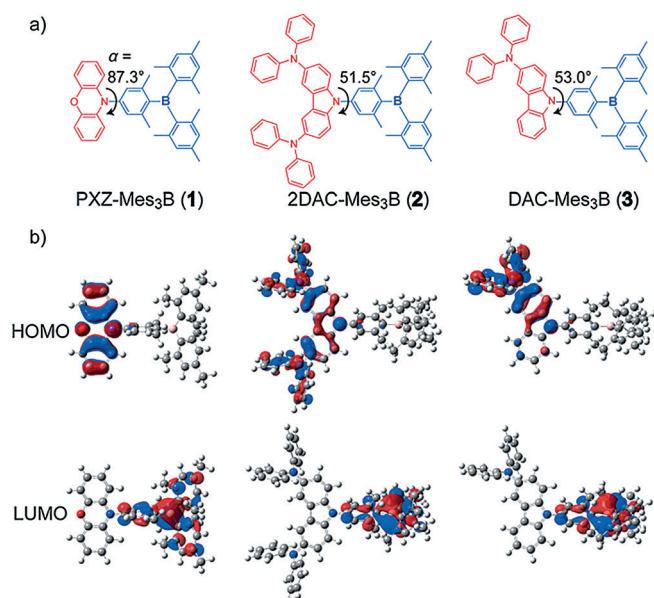


Figure 1. a) Molecular structures of triarylboron emitters. Torsion angles between donor and acceptor units, α , are also shown. b) Calculated HOMO and LUMO distributions of **1–3**. Surface isovalue: $\pm 0.03 a_0^{-3/2}$.

We performed the geometry optimization of **1–3** at the PBE0/6-31G(d) level using density functional theory (DFT) implemented in the Gaussian09 program package.^[15] The optimized structures of **1–3** show that **1** has a larger torsion angle (α) between the donor unit and adjacent phenyl ring than **2** and **3** because of steric repulsion arising from the H atoms at the 1,9-positions of PXZ and those on the neighboring phenyl ring (Table 1). The HOMO and LUMO

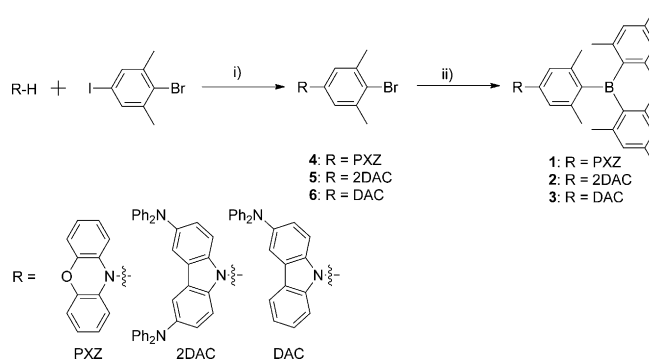
Table 1: Calculated and experimental properties of **1–3**.

Compound	Calculation			Experiment ^[a]		
	α ^[b] [°]	f ^[c]	ΔE_{ST} ^[d] [meV]	λ_{abs} ^[e] [nm]	λ_{PL} ^[f] [nm]	Φ_{PL} ^[g] [%]
1	87.3	0.0002	8	399	509	44
2	51.5	0.0995	21	387	495	84
3	53.0	0.0838	19	375	477	91

[a] Measured in O₂-free toluene (1×10^{-5} M) at r.t. [b] Torsion angle between the donor unit and adjacent phenyl ring. [c] Oscillator strength. [d] Calculated energy gap between S₁ and T₁. [e] UV/Vis absorption maximum wavelength. [f] PL emission maximum wavelength. [g] Photoluminescence quantum yield (PLQY).

of **1–3** are mainly distributed on the electron-donating units and electron-accepting Mes₃B unit, respectively, indicating efficient separation of HOMO and LUMO (Figure 1b). The overlap of the HOMO and LUMO of **1** is smaller than those of **2** and **3**. The difference of HOMO–LUMO overlap, which is closely related to α , affects ΔE_{ST} and the oscillator strength (f) of **1–3**.^[16] Time-dependent (TD)-DFT calculations^[17] at the PBE0/6-31G(d) level using the Gaussian09 program package^[15] show that ΔE_{ST} and f of **1** are smaller than those of **2** and **3** (Table 1).

Compounds **1–3** were synthesized according to Scheme 1. Bromo-substituted precursors **4–6** were synthesized by copper-catalyzed Ullmann coupling of 2-bromo-5-iodo-1,3-dimethylbenzene with corresponding amine-based donor units. Lithiation of **4–6** in ether or cyclopentyl methyl ether and subsequent treatment with dimesitylboron fluoride gave **1–3** in overall yields of 39–61%.



Scheme 1. Preparation of triarylboron complexes **1–3**. Reagents/conditions: i) CuI, L-proline, DMSO, K₂CO₃, 110°C; ii) *n*BuLi, dimesitylboron fluoride, Et₂O or cyclopentyl methyl ether, 0°C to r.t.

Figure 2a shows steady-state UV/Vis absorption and photoluminescence (PL) spectra of **1–3** in toluene; photo-physical data of **1–3** are given in Table 1. The compounds show absorption peaks (λ_{abs}) around 380 nm, and broad structureless PL spectra with emission peaks (λ_{PL}) in the green to sky-blue region (Table 1). The DFT and TD-DFT calculations indicate that the absorptions of **1–3** result from ICT transitions, owing to their spatially separated HOMO and LUMO (Figure 1b; Supporting Information, Table S1). Their ICT characters were supported by the absorption and PL spectra of **1–3** in various solutions; the absorption spectra were almost independent of solvent polarity (Supporting Information, Figure S1), whereas the PL spectra showed large red shifts with solvent polarity being increased (Figure S2).

Figure 2b shows PL spectra of **1–3** in host matrices. The green emitter **1** (T₁ level = 2.40 eV) was doped in 4,4'-di(9H-

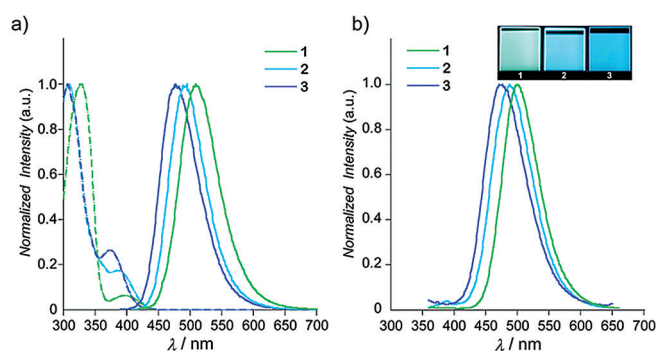


Figure 2. a) Normalized UV/Vis absorption (dashed lines) and PL (solid lines) spectra of **1** (green), **2** (sky-blue), and **3** (blue) in toluene solution (1.0×10^{-5} M). b) Normalized PL spectra of **1** (green) doped in CBP (16 wt%), and **2** (sky-blue) and **3** (blue) doped in DPEPO (16 wt%).

carbazol-9-yl)-1,1'-biphenyl (CBP, $T_1 = 2.58$ eV). Sky-blue emitters **2** ($T_1 = 2.51$ eV) and **3** ($T_1 = 2.54$ eV) were doped in bis[2-(diphenylphosphino)phenyl]ether oxide (DPEPO, $T_1 = 3.00$ eV) to prevent back transfer of excited energy from guest to host.^[18] The PL spectra of these films only show the fluorescence of the dopants, suggesting efficient energy transfer from the host to the guest molecules (Figure 2b).

Photoluminescence quantum yields (Φ_{PL}) of **1–3** in oxygen (O_2)-free toluene (**1**: $\Phi_{PL} = 44\%$; **2**: 84% ; **3**: 91%) were larger than those of as-prepared solutions containing O_2 (**1**: $\Phi_{PL} = 20\%$; **2**: 51% ; **3**: 54%). This is because some T_1 excitons transferred from S_1 to T_1 by intersystem crossing (ISC) are quenched by dissolved O_2 , so $T_1 \rightarrow S_1$ RISC is inhibited.^[10a,11b,c]

The highest Φ_{PL} of **1–3** doped in host matrices (16 wt %, CBP for **1**, DPEPO for **2** and **3**) were 92 %, 100 %, and 87 %, respectively, at room temperature (Table 2).

Table 2: OLED and photophysical properties of 16 wt % guest:host films of **1–3**.

Film	$\eta_{EQE}^{[a]}$ [%]	CIE ^[b] [x, y]	$\lambda_{EL}^{[c]}$ [nm]	$\lambda_{PL}^{[d]}$ [nm]	$\Phi_{PL}^{[e]}$ [%]	$\Delta E_{ST}^{[f]}$ [meV]
1:CBP	22.8	0.22, 0.55	502	504	92	71 ± 6
2:DPEPO	21.6	0.18, 0.43	492	487	100	58 ± 21
3:DPEPO	14.0	0.17, 0.30	488	477	87	62 ± 23

[a] Maximum external quantum efficiency. [b] CIE coordinate. [c] EL emission maximum wavelength. [d] PL emission maximum wavelength. [e] PLQY. [f] Energy gap between S_1 and T_1 .

Up-conversion from T_1 to S_1 was confirmed by transient PL decay measurements of **1–3** in host matrices (Figures 3 and S3). For **1**, delayed PL decay components were observed in both O_2 -free toluene and CBP (Figure 3). In contrast, **2** and **3** exhibited small amounts of delayed PL components both in O_2 -free toluene and host matrices, reflecting large f values (Table 1 and Figure S3).

ΔE_{ST} values were evaluated from Arrhenius plots of rate constants for RISC (k_{RISC}).^[11c] We obtained similar ΔE_{ST} for **1–3** in host matrices (Table 2), which are close to that of one of the most efficient TADF emitters, 1,2,3,5-tetrakis(carbazol-9-yl)-4,6-dicyanobenzene (4CzIPN: $\Delta E_{ST} = 83$ meV).^[11c] The experimental errors of ΔE_{ST} for **2** and **3** were large because of the small fraction of their delayed components, especially at low temperature.

We evaluated the performance of OLEDs using 16 wt % of **1–3** in host matrices as emitting layer (Figures 4 and S4). Figure 4a shows device structures (for detail of device fabrications, see the Supporting Information, Figures S5 and S6). The electroluminescence (EL) emission peaks (λ_{EL}) of devices **I–III** were observed in the green to sky-blue region (Figure 4b and Table 2). No other emission from host materials or any other layers was observed for devices **I–III**, suggesting that all excitons generated in the devices are effectively confined in the emitting layers. The Commission Internationale de L'Eclairage (CIE) coordinates of devices **II** and **III** (Table 2) are close to those of OLEDs using the typical sky-blue phosphorescent emitter bis[2-(4,6-difluorophenyl)pyridinato-C2,N](picolinato)iridium(III) (FIrpic).^[19]

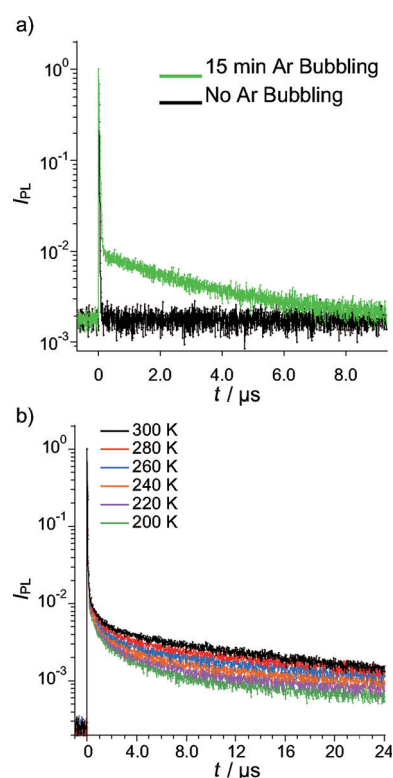


Figure 3. a) Transient PL decay characteristics of **1** in toluene (1.0×10^{-5} M) at room temperature. b) Temperature dependence of transient PL decays of **1** doped in CBP (16 wt %).

Figure 4c reveals that the maximum η_{EQE} of devices **I**, **II**, and **III** were 22.8 %, 21.6 %, and 14.0 %, respectively, far higher than the theoretical limit for conventional fluorescent emitters (5–7.5 %), indicating that efficient up-conversion of excitons from T_1 to S_1 is realized in these devices. In particular, device **I** showed low efficiency roll-off (Figure 4c); its η_{EQE} remains extremely large even at practical luminance levels, with values of 19.1 % at 500 cd m^{-2} (for display applications) and 14.2 % at 3000 cd m^{-2} (for lighting applications).

In conclusion, we synthesized TAB-based OLED emitters **1–3** that achieved both high Φ_{PL} and low ΔE_{ST} . A sky-blue OLED using **2** as an emitter exhibited a maximum η_{EQE} of 21.6 %, the highest value for a TADF-based blue OLED.^[13] A green OLED with **1** as an emitter showed η_{EQE} of 22.8 %, which is the highest for an OLED with a TAB emitter to date. These high η_{EQE} are attributed to TADF emission originating from efficient up-conversion from T_1 to S_1 . Further modification of D-A TAB-based TADF frameworks will provide OLEDs with enhanced performance and full-color tuning.

Acknowledgements

This work was supported by a Japan Society and the Promotion of Science (JSPS) Grant-in-Aid for JSPS Fellows (No. 14J04794), and JSPS Grant-in-Aid for Scientific Research (A). This work was also supported by the Collaborative Research Program of Institute for Chemical

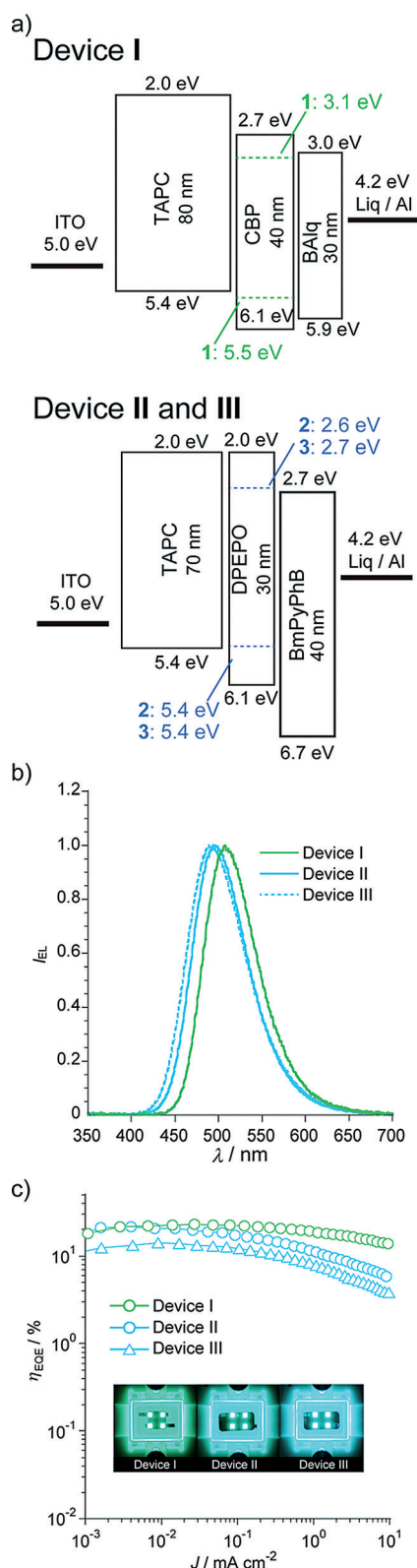


Figure 4. a) Structures and energy band diagrams, b) EL spectra at 100 cd m⁻², and c) η_{EQE} -current density characteristics of devices I-III.

Research, Kyoto University (Grant No. 2015-14). Computation time on a supercomputer system was provided by the Institute for Chemical Research, Kyoto University, Japan, and

the Academic Center for Computing and Media Studies (ACCMS), Kyoto University, Japan. NMR measurements were supported by the Joint Usage/Research Center (JURC) at the Institute for Chemical Research, Kyoto University, Japan.

Keywords: boron · donor-acceptor systems · electroluminescence · fluorescence · organic light-emitting diodes

How to cite: *Angew. Chem. Int. Ed.* **2015**, *54*, 15231–15235
Angew. Chem. **2015**, *127*, 15446–15450

- [1] a) C. D. Entwistle, T. B. Marder, *Chem. Mater.* **2004**, *16*, 4574–4585; b) R. Stahl, C. Lambert, C. Kaiser, R. Wortmann, R. Jakober, *Chem. Eur. J.* **2006**, *12*, 2358–2370; c) A. Wakamiya, K. Mori, S. Yamaguchi, *Angew. Chem. Int. Ed.* **2007**, *46*, 4273–4276; *Angew. Chem.* **2007**, *119*, 4351–4354; d) Z. M. Hudson, S. Wang, *Acc. Chem. Res.* **2009**, *42*, 1584–1596.
- [2] C. D. Entwistle, T. B. Marder, *Angew. Chem. Int. Ed.* **2002**, *41*, 2927–2931; *Angew. Chem.* **2002**, *114*, 3051–3056.
- [3] a) S. Yamaguchi, S. Akiyama, K. Tamao, *J. Am. Chem. Soc.* **2001**, *123*, 11372–11375; b) T. W. Hudnall, C.-W. Chiu, F. P. Gabbaï, *Acc. Chem. Res.* **2009**, *42*, 388–397.
- [4] G. C. Welch, R. R. San Juan, J. D. Masuda, D. W. Stephan, *Science* **2006**, *314*, 1124–1126.
- [5] a) Y. Shirota, M. Kinoshita, T. Noda, K. Okumoto, T. Ohara, *J. Am. Chem. Soc.* **2000**, *122*, 11021–11022; b) H. Doi, M. Kinoshita, K. Okumoto, Y. Shirota, *Chem. Mater.* **2003**, *15*, 1080–1089; c) W. L. Jia, M. J. Moran, Y.-Y. Yuan, Z. H. Lu, S. Wang, *J. Mater. Chem.* **2005**, *15*, 3326–3333; d) W. L. Jia, X. D. Feng, D. R. Bai, Z. H. Lu, S. Wang, G. Vamvounis, *Chem. Mater.* **2005**, *17*, 164–170; e) S.-L. Lin, L.-H. Chan, R.-H. Lee, M.-Y. Yen, W.-J. Kuo, C.-T. Chen, R.-J. Jeng, *Adv. Mater.* **2008**, *20*, 3947–3952; f) F. Li, W. Jia, S. Wang, Y. Zhao, Z.-H. Lu, *J. Appl. Phys.* **2008**, *103*, 034509; g) A. Shuto, T. Kushida, T. Fukushima, H. Kaji, S. Yamaguchi, *Org. Lett.* **2013**, *15*, 6234–6237.
- [6] M. Pope, H. P. Kallmann, P. Magnante, *J. Chem. Phys.* **1963**, *38*, 2042–2043.
- [7] a) L. H. Smith, J. A. E. Wasey, W. L. Barnes, *Appl. Phys. Lett.* **2004**, *84*, 2986–2988; b) D. Tanaka, H. Sasabe, Y. J. Li, S. J. Su, T. Takeda, J. Kido, *Jpn. J. Appl. Phys.* **2007**, *46*, L10–L12.
- [8] a) M. A. Baldo, D. F. O'Brien, Y. You, A. Shoustikov, S. Sibley, M. E. Thompson, S. R. Forrest, *Nature* **1998**, *395*, 151–154; b) C. Adachi, M. A. Baldo, M. E. Thompson, S. R. Forrest, *J. Appl. Phys.* **2001**, *90*, 5048–5051; c) H. Sasabe, J. Kido, *Eur. J. Org. Chem.* **2013**, 7653–7663.
- [9] a) Z. M. Hudson, C. Sun, M. G. Helander, H. Amarné, Z.-H. Lu, S. Wang, *Adv. Funct. Mater.* **2010**, *20*, 3426–3439; b) Z. B. Wang, M. G. Helander, Z. M. Hudson, J. Qiu, S. Wang, Z. H. Lu, *Appl. Phys. Lett.* **2011**, *98*, 213301; c) X. Wang, Y.-L. Chang, J.-S. Lu, T. Zhang, Z.-H. Lu, S. Wang, *Adv. Funct. Mater.* **2014**, *24*, 1911–1927.
- [10] a) A. Endo, K. Sato, K. Yoshimura, T. Kai, A. Kawada, H. Miyazaki, C. Adachi, *Appl. Phys. Lett.* **2011**, *98*, 083302; b) T. Nakagawa, S.-Y. Ku, K.-T. Wong, C. Adachi, *Chem. Commun.* **2012**, *48*, 9580–9582.
- [11] a) H. Tanaka, K. Shizu, H. Miyazaki, C. Adachi, *Chem. Commun.* **2012**, *48*, 11392–11394; b) G. Méhes, H. Nomura, Q. Zhang, T. Nakagawa, C. Adachi, *Angew. Chem. Int. Ed.* **2012**, *51*, 11311–11315; *Angew. Chem.* **2012**, *124*, 11473–11477; c) H. Uoyama, K. Goushi, K. Shizu, H. Nomura, C. Adachi, *Nature* **2012**, *492*, 234–238; d) K. Sato, K. Shizu, K. Yoshimura, A. Kawada, H. Miyazaki, C. Adachi, *Phys. Rev. Lett.* **2013**, *110*, 247401; e) S. Hirata, Y. Sakai, K. Masui, H. Tanaka, S. Y. Lee, H. Nomura, N. Nakamura, M. Yasumatsu, H. Nakanotani, Q.

- Zhang, K. Shizu, H. Miyazaki, C. Adachi, *Nat. Mater.* **2015**, *14*, 330–336; f) H. Kaji, H. Suzuki, T. Fukushima, K. Shizu, K. Suzuki, S. Kubo, T. Komino, H. Oiwa, F. Suzuki, A. Wakamiya, Y. Murata, C. Adachi, *Nat. Commun.* **2015**, *6*, 8476.
- [12] a) M. Numata, T. Yasuda, C. Adachi, *Chem. Commun.* **2015**, *51*, 9443–9446; b) Y. Kitamoto, T. Namikawa, D. Ikemizu, Y. Miyata, T. Suzuki, H. Kita, T. Sato, S. Oi, *J. Mater. Chem. C* **2015**, *3*, 9122–9130; c) H. Hirai, K. Nakajima, S. Nakatsuka, K. Shiren, J. Ni, S. Nomura, T. Ikuta, T. Hatakeyama, *Angew. Chem. Int. Ed.* **2015**, *54*, 13581–13585; *Angew. Chem.* **2015**, *127*, 13785–13789.
- [13] During the submission of this paper, Kim's group reported blue TADF OLED with η_{EQE} of 22.3%. J. W. Sun, J. Y. Baek, K.-H. Kim, C.-K. Moon, J.-H. Lee, S.-K. Kwon, Y.-H. Kim, J.-J. Kim, *Chem. Mater.* **2015**, *27*, 6675–6681.
- [14] N. J. Turro, V. Ramamurthy, J. C. Sciano, *Modern Molecular Photochemistry of Organic Molecules*, University Science Books, Sausalito, **2010**.
- [15] Gaussian09, Revision C.01, M. J. Frisch, G. et al., Gaussian, Inc., Wallingford, CT, USA, **2009**.
- [16] a) K. Shizu, J. Lee, H. Tanaka, H. Nomura, T. Yasuda, H. Kaji, C. Adachi, *Pure Appl. Chem.* **2015**, *87*, 627–638; b) K. Shizu, H. Tanaka, M. Uejima, T. Sato, K. Tanaka, H. Kaji, C. Adachi, *J. Phys. Chem. C* **2015**, *119*, 1291–1297.
- [17] a) R. Bauernschmitt, R. Ahlrichs, *Chem. Phys. Lett.* **1996**, *256*, 454–464; b) M. E. Casida, C. Jamorski, K. C. Casida, D. R. Salahub, *J. Chem. Phys.* **1998**, *108*, 4439–4449.
- [18] C. Han, Y. Zhao, H. Xu, J. Chen, Z. Deng, D. Ma, Q. Li, P. Yan, *Chem. Eur. J.* **2011**, *17*, 5800–5803.
- [19] S. O. Jeon, J. Y. Lee, *J. Mater. Chem.* **2012**, *22*, 4233–4243.

Received: September 4, 2015

Revised: October 19, 2015

Published online: November 13, 2015